Appl. Magn. Reson. 27, 267–278 (2004)

Applied Magnetic Resonance

Magnetic Anisotropy of the $SrCu_2(BO_3)_2$ System as Revealed by X-Band ESR

A. Zorko[1], D. Arčon[1], H. Kageyama[2], and A. Lappas[3]

[1] Jožef Stefan Institute, Ljubljana, Slovenia
[2] Department of Chemistry, Graduate School of Science, Kyoto University, Kyoto, Japan
[3] Institute of Electronic Structure and Laser, Foundation for Research and Technology Hellas, Heraklion, Greece

Received October 3, 2003

Abstract. X-band electron paramagnetic resonance measurements on a single crystal of the highly frustrated $SrCu_2(BO_3)_2$ system are shown to provide an essential inspection of the magnetic anisotropy present in this compound. The very broad absorption lines seem to be consistent with the largest anisotropy term, namely, the antisymmetric Dzyaloshinsky-Moriya (DM) interaction allowed by symmetry. However, the previously well-accepted model of only interdimer interaction is generalized with additional intradimer DM terms. Moreover, spin-phonon coupling is recognized as the cause of the line width broadening with increasing temperature.

1 Introduction

Low-dimensional spin-gap systems with quantum-disordered singlet ground state have been in the mainstream of scientific research in the last decade due the diversity of possible ground state phases and richness of low-lying magnetic excitation spectra. The gap in magnetic excitation spectrum (spin gap) is a common feature in one-dimensional (1-D) antiferromagnets and is usually triggered by competing exchange interactions or dimerization present in the system. On the contrary, the field of spin-gap systems in two dimensions is not nearly as rich as in one dimension since the general characteristic of 2-D antiferromagnets is a tendency to exhibit 3-D order at lower temperatures due to interlayer exchange interactions. However, sufficient frustration provided by a special exchange topology of the system can resolve the nonmagnetic singlet state as the ground state of the system and is thus directly responsible for the opening of the spin gap.

$SrCu_2(BO_3)_2$ with localized $S = 1/2$ Cu^{2+} spins is one of the few 2-D systems exhibiting a spin-gap behavior [1]. Already in the early stages [2] this

system was recognized as the first chemical realization of a model proposed by Shastry and Sutherland [3], which takes into account 2-D square lattice of antiferromagnetically coupled spins with additional selected diagonal bonds. The Hamiltonian of the investigated system is thus given by

$$\mathcal{H}_{\mathrm{ex}} = J\sum_{(ij)}\mathbf{S}_i\mathbf{S}_j + J'\sum_{(lm)}\mathbf{S}_l\mathbf{S}_m, \qquad (1)$$

where (ij) terms represent nearest-neighbor (nn) exchange coupling pairs while (lm) stands for next-nearest-neighbor (nnn) pairs of spins with exchange constants estimated to be $J = 85$ K and $J' = 54$ K [4]. The unique network of orthogonal interacting dimers composed of Cu^{2+} ions is shown as the inset to Fig. 1. The ground state of the system remains a simple product of spin singlets on each dimer even if interlayer exchange coupling $J'' = 8$ K is taken into account [5], which makes the J'-coupling extremely frustrated. As a result of the inherent geometrical frustration the lowest lying magnetic excitation – a single triplet excitation present on one of the dimers – is extremely localized as evidenced by almost dispersionless excitation band [6] and relatively small value of the spin gap $\Delta = 34$ K with respect to the exchange coupling constant J [6, 7].

The singlet-triplet excitation possesses another remarkable property, namely, a fine structure as revealed for the first time by a high-field electron spin resonance (ESR) experiment [7]. The interpretation of high-field ESR spectra was, in fact, quite an achievement as far as the understanding of magnetic anisotropy

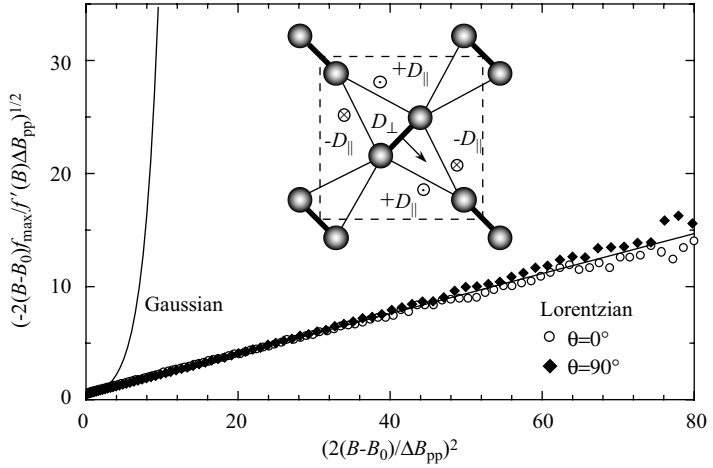

Fig. 1. Line shape analysis for X-band absorption lines of $SrCu_2(BO_3)_3$ single crystal for external magnetic field applied parallel (open circles) and perpendicular (full diamonds) to crystal c-axis at 525 K. Solid lines correspond to absorption profiles of Lorentzian and Gaussian type. The inset shows the 2-D network of Cu^{2+} ions, with thick lines representing the nn exchange coupling J and thin lines related to the nnn exchange J'. The direction of interdimer $D_{\|}$ as well as intradimer $D_{\perp}$ DM interaction is also presented.

of the system is concerned. The experimental singlet-triplet transitions are forbidden due to the fact that the Shastry-Sutherland exchange Hamiltonian commutes with a magnetic dipole operator. Such transitions can be explained only by including spin-anisotropy terms to the original Hamiltonian, which are then responsible for mixing a small amount of excited states into the ground singlet state. A feasible analysis of the observed angular-dependent fine structure was proposed by Cépas et al. [8] with the introduction of antisymmetric anisotropic exchange interaction, known as Dzyaloshinsky-Moriya (DM) interaction of the form

$$\mathcal{H}_{\mathrm{DM}} = \sum_{(ij)}\pm D_{\|}\,\mathbf{e}_c\mathbf{S}_i \times \mathbf{S}_j. \qquad (2)$$

Such antisymmetric interaction is quite common in highly anisotropic, i.e., low-dimensional systems, with large exchange coupling and no center of inversion between interacting spins. It is the first-order perturbation effect of spin-orbit coupling and can often be by far the largest anisotopic term of the Hamiltonian. The magnitude of the DM interaction can be estimated from the g-shift and exchange constant, $D \sim \Delta g/gJ'$. As the Cu-B-O planes are almost flat [9], only interdimer DM interaction was employed with DM vectors $D_{\|} = 2.1$ K [8] pointing in the crystal c-direction (inset to Fig. 1), due to symmetry arguments originally proposed by Moriya [10].

Magnetic anisotropy determines the spin dynamics in the system and is thus reflected in ESR spectra through the observed line widths and lineshifts. To establish the nature of the largest anisotropic terms, we previously conducted X-band ESR measurements on a powdered sample of $SrCu_2(BO_3)_2$ and concluded that symmetric anisotropic exchange and/or antisymmetric DM interaction had to be considered in order to justify the observed broad spectra [11]. However, performing experiments on single crystals offers an additional insight into the anisotropy of the system. Namely, the angular dependence of the line width can yield supplementary information on the direction of anisotropy axes in addition to the magnitude of anisotropic contributions. Moreover, the presence of diffusive motion of spins can be verified through the enhanced contributions of secular parts of anisotropic terms. Measurements on single crystals thus often allow one to rule out particular anisotropy terms in favor of other ones. Performing X-band ESR on a single crystal of $SrCu_2(BO_3)_2$ hence seems a reasonable way to verify the validity of the picture of spin dynamics proposed for this particular system. Furthermore, it can yield information on additional anisotropic terms which have not yet been evaluated or even observed by other spectroscopic techniques.

2 Material and Methods

A single crystal of $SrCu_2(BO_3)_2$ was grown by the travelling solvent floating zone (TSFZ) method from a polycrystalline $SrCu_2(BO_3)_2$ powder with $LiBO_2$ as a solvent [12]. The direction of crystal axes was determined by means of X-ray scattering and the high purity was verified by almost no low-temperature Curie-like

upturn of the magnetic susceptibility down to 2 K. A crystal of a size of 5 by 2 by 2 mm was used for ESR experiments.

X-band ESR measurements were performed on a commercially available Bruker E580 FT/CW spectrometer working at a Larmor frequency of $\nu_L = 9.5$ GHz. The temperature of 525 K was reached using high-temperature controller with preheated-nitrogen-flow cryostat.

3 Results and Discussion

Angular-dependent X-band ESR spectra on a single crystal of $SrCu_2(BO_3)_2$ were recorded at 295 and 525 K, i.e., at two temperatures well above the characteristic intradimer exchange temperature $J = 85$ K. Bearing in mind that the $\mathcal{H}_0 = \mathcal{H}_z + \mathcal{H}_{ex}$ part of the total spin Hamiltonian $\mathcal{H} = \mathcal{H}_0 + \mathcal{H}'$ is dominant, the anisotropic part $\mathcal{H}'$ can be treated as a perturbation and the Kubo-Tomita approach to magnetic resonance should be justified at such high temperatures [13]. Here, the $\mathcal{H}_z$ and $\mathcal{H}_{ex}$ terms represent the Zeeman and isotropic exchange (Eq. (1)) parts of the Hamiltonian, respectively. As we are dealing with $S = 1/2$ spins, no single-spin anisotropy terms are present. So the magnetic anisotropy is in principle driven by the dipolar interactions $\mathcal{H}_{dd}$ between neighboring magnetic moments, the hyperfine coupling $\mathcal{H}_{hf}$ of electron spins with nuclear spins, the symmetric anisotropic exchange interaction $\mathcal{H}_{ae}$ (pseudo-dipolar interaction) and the antisymmetric DM interaction $\mathcal{H}_{DM}$, i.e.,

$$\mathcal{H}' = \mathcal{H}_{dd} + \mathcal{H}_{hf} + \mathcal{H}_{ae} + \mathcal{H}_{DM}. \quad (3)$$

The absorption lines should be extremely exchange narrowed as the isotropic exchange is by far the superior interaction present in the investigated system ($k_B J \gg g\mu_B B_0 \sim g\mu_B \Delta B_{pp}$). In this regime, the peak-to-peak line width is given by the expression [14]

$$\Delta B_{pp} \approx \frac{2}{\sqrt{3}} \frac{k_B^2}{\hbar g \mu_B} \frac{M_2}{\omega_{eff}} \approx \frac{2}{\sqrt{3}} \frac{k_B}{g\mu_B} \frac{M_2}{J}, \quad (4)$$

where $\omega_{eff} = k_B J/\hbar$ is the characteristic frequency of the exchange modulation and M_2 is the second moment given by

$$M_2 = \langle [H', S_+][S_-, H'] \rangle / \langle S_+ S_- \rangle.$$

The line shape is expected to be Lorentzian. However, line broadening and deviations from Lorentzian profiles are often detected in low-dimensional systems at higher temperatures due to spin diffusion [15].

The standard analysis of the line shape of ESR absorption spectra for $SrCu_2(BO_3)_2$ for both the parallel and the perpendicular direction of the external magnetic field B_0, with respect to the crystal anisotropy c-axis, is shown in Fig. 1 for $T = 525$ K. In the plot $(-(B - B_0)f_{max}/f'(B)\Delta B_{pp})^{1/2}$ vs. $(2(B - B_0)/\Delta B_{pp})^2$ Lorentzian profiles yield a linear dependence, while Gaussian lines produce a much faster (exponentially) increasing function due to the rapid decrease of the signal in the tails of resonant absorption spectra. Here, $f'(B)$ represents the derivative absorption spectrum with peaks $\pm f'_{max}$. Spin diffusion results in a function somewhere in-between the two extreme cases [16]. As it can be seen from Fig. 1 the presence of spin diffusion can be excluded from the $SrCu_2(BO_3)_2$ system as the absorption profiles obey Lorentzian dependence.

3.1 g-Factor Anisotropy

Next we focus on the anisotropy of the g-factor presented in Fig. 2 for $T = 295$ K. As expected from the crystal structure [9], the g-tensor is axially symmetric with a pronounced angular dependence in the ac-plane (θ-dependence) and only a minor dependence with respect to the azimuthal angle ϕ (ab-plane). Fitting the θ-dependence to the equation

$$g = \sqrt{g_\parallel^2 \cos^2\theta + g_\perp^2 \sin^2\theta} \quad (5)$$

yields parallel and perpendicular g-factors with respect to the c-axis: $g_\parallel = 2.269 \pm 0.002$ and $g_\perp = 2.057 \pm 0.002$. Such g-shifts are common for Cu^{2+} $3d^9$ configuration where the crystal field is stronger than the spin-orbit coupling [17,

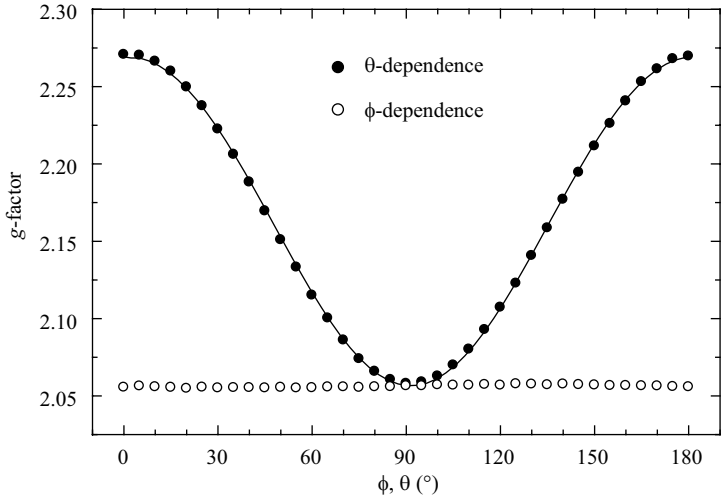

Fig. 2. Anisotropy of the g-tensor of the X-band ESR spectra for the $SrCu_2(BO_3)_3$ single crystal in the crystal ac-plane (θ-dependence; full circles) and in the ab-plane (ϕ-dependence; open circles) at 295 K. The fit (solid line) corresponds to Eq. (5).

p. 48]. Crystal field thus effectively quenches orbital motion producing an effective spin of 1/2 for the ion. Orbital moments are partially restored by spin-orbit coupling leading to g-shifts. The anisotropy of the g-shifts in the ab-plane is much smaller. It can be limited by experimental accuracy to a value smaller than 0.002. At 525 K, the g-factor shows virtually the same angular dependence with unchanged eigenvalues.

3.2 Spin-Anisotropy Contributions to Line Widths

Line widths of the X-band ESR spectra at 295 and 525 K are presented in Fig. 3. As already emphasized [11] all the anisotropic terms included in the Hamiltonian Eq. (3) have to be considered in determination of the contributions to the ESR line width. Furthermore, the Lorentzian line shape of absorption spectra confirms the assumption of the presence of strong exchange narrowing, so that the use of Eq. (4) is well justified. Following the previous estimates of the dipolar and hyperfine contribution to the second moment $M_2^{\mathrm{dd}} \approx (g\mu_B/k_B 1000\ \mathrm{G})^2$ and $M_2^{\mathrm{hf}} \approx (g\mu_B/k_B 200\ \mathrm{G})^2$ [11], line widths of the order of $\Delta B_{\mathrm{pp}}^{\mathrm{dd}} \approx 2$ G and $\Delta B_{\mathrm{pp}}^{\mathrm{hf}} \approx 0.1$ G are expected, which are several orders of magnitude smaller than the experimental values. Employing symmetric anisotropic exchange, which is a result of second-order perturbation of the spin-orbit coupling (its amplitude can be evaluated as $AE \sim (\Delta g/g)^2 J = 1.0$ K), and antisymmetric DM interaction yields the second moment of the form [18]

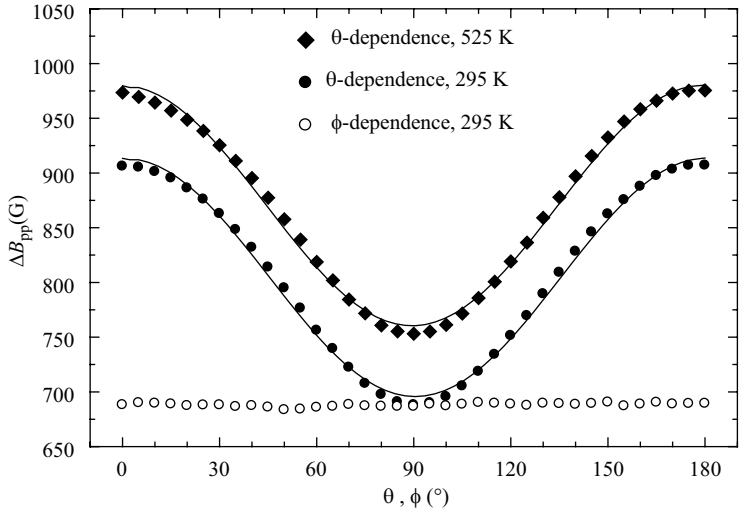

Fig. 3. Line width anisotropy of the X-band ESR absorption lines for the $SrCu_2(BO_3)_3$ single crystal in the crystal ac-plane (full symbols) at 295 K (circles) and 525 K (diamonds) and in the ab-plane at 295 K (open circles). Experimental data is fitted to equation of the form $A + B\cos^2\theta$ (solid lines).

$$M_2^{\mathrm{ae,DM}} = \frac{S(S+1)}{3N}\left(2\sum_{(ij)} AE^2 + \sum_{(lm)}\left[(D_{lm}^x)^2 + (D_{lm}^y)^2 + 2(D_{lm}^z)^2\right]\right), \quad (6)$$

where the components of the DM vector are given in the laboratory frame with the z-axis pointing in the direction of the external magnetic field B_0. With Eqs. (4) and (6) the contribution of the symmetric part can be evaluated as $\Delta B_{\mathrm{pp}}^{\mathrm{ae}} \approx k_B AE^2/2\sqrt{3}g\mu_B J \approx 30$ G, while the antisymmetric DM interaction gives a value of $\Delta B_{\mathrm{pp}}^{\mathrm{DM}} \approx 2k_B D^2/\sqrt{3}g\mu_B J \approx 460$ G taking into account the interdimer DM interaction $D_{||} = 2.1$ K as proposed in ref. 8.

The above analysis favors the DM interaction as the only candidate capable of inducing sufficiently large line widths, as observed in the current experiment. This conclusion could have been already reached by conducting the experiment on the powdered sample, where the room temperature peak-to-peak line width was around 760 G. However, the fundamental advantage of the present single-crystal experiment is the power to test the proposed picture of magnetic anisotropy in the $SrCu_2(BO_3)_2$ system given by Eq. (2) through the angular dependence of the observed line widths. This can in fact yield additional information about the direction of DM vectors as discussed below.

3.3 Line Width Anisotropy Determined by DM Interaction

Let the external magnetic field B_0 have an arbitrary orientation described by the polar angle θ with respect to the crystal c-axis and the azimuthal angle ϕ in the ab-plane. Applying the transformation of the DM vector from laboratory frame to crystal frame gives the expression of the angular dependence of the DM second moment

$$\begin{aligned} M_2^{\mathrm{DM}} = {} & \frac{S(S+1)}{3N} \\ & \times \sum_{(lm)}\Big\{(D_{lm}^a)^2(1+\sin^2\theta\cos^2\phi) + (D_{lm}^b)^2(1+\sin^2\theta\sin^2\phi) + (D_{lm}^c)^2(1+\cos^2\theta) \\ & + 2D_{lm}^a D_{lm}^b \sin^2\theta\sin\phi\cos\phi + 2D_{lm}^a D_{lm}^c \sin\theta\cos\theta\cos\phi \\ & + 2D_{lm}^b D_{lm}^c \sin\theta\cos\theta\sin\phi\Big\}. \end{aligned} \quad (7)$$

Entering only the interdimer DM interaction $\mathbf{D} = (0,0,D_{||})$ into Eq. (7) yields the angular dependence of the second moment of the form $M_2^{\mathrm{DM}} \propto 1 + \cos^2\theta$. However, the angular dependence of the observed line width at 295 and 525 K is significantly different from this prediction (Fig. 3). θ-dependence can be well described by an equation of the form $A + B(1 + \cos^2\theta)$ with A and B contributions of the same order of magnitude. The parameters thus obtained are $A = 478 \pm 5$ G, $B = 218 \pm 5$ G for room temperature and $A = 541 \pm 5$ G, $B = 220 \pm 5$ G for the higher temperature. The angular-dependent part B is temperature inde-

pendent and coincides very well with the order-of-magnitude prediction of 460 G at $\theta = 0°$, which should be asymptotically approached when going to infinite temperature. However, unexpectedly, there is an additional term A, which is of the same amplitude as the B term. In contrast to B, A is T-dependent. The magnetic anisotropy introducing such contribution to the line width should be quite strong as the amplitudes of A and B terms are virtually the same. The symmetric-anisotropy-interaction contribution ΔB_{pp}^{ae} can be excluded for at least two reasons. The first one is pointed out by the above order-of-magnitude calculation and the second one is due to the characteristic angular dependence of this interaction [19]. Namely, symmetric anisotropic exchange interaction can be presented by a traceless tensor whose principal axes coincide with those of the g-tensor. As the $SrCu_2(BO_3)_2$ system is axially symmetric to a very good approximation, with the anisotropy axis pointing in the crystal c-direction, the contribution of H_{ae} to the line width is expected to vary with the orientation of external magnetic field according to $M_2^{ae} \propto 1 + \cos^2\theta$. This is the same angular dependence as provided by DM interdimer interaction with DM vectors perpendicular to the ab-plane and as such cannot provide an adequate explanation of the additional A term observed in the experiment.

We propose that the origin of the experimental angular dependence of the line width lies in additional magnetic-anisotropy terms of the DM type. Although, in the first approximation, treating the crystal ab-plane as strictly planar, DM vectors are obliged to point into the c-direction and no intradimer interaction is allowed due to symmetry reasons, one can loosen these constraints if a buckling of the ab-planes is taken into account [20]. Bending of neighboring CuO_4 plaquettes forming dimers suppresses inversion symmetry within dimers thus allowing finite intradimer DM interaction $D_\perp$. In addition, also a finite in-plane component of interdimer interactions D_{ab} is endorsed. In fact, it has been recently reported that the latter interaction is responsible for the observed anomalies in high-resolution inelastic neutron scattering experiments [21]. A sizable in-plane interdimer component of the order of 30% of $D_\parallel$ was suggested. The ESR line width is proportional to the square of the amplitude of DM vector, which would imply that the corrections of the D_{ab} term amount in a correction of only about 10% of the contribution to the line width due to $D_\parallel$ interaction. However, the observed effect in our experiment is much larger.

The behavior of the line width in the ab-plane is less exciting as there is virtually no ϕ-dependence (Fig. 3). The line widths seem to be randomly scattered as a function of the azimuthal angle with the amplitude of 5 G around the value of 686 G. Such behavior corresponds to the addition of intradimer DM interaction since in this case the DM vectors are forced to lie in the ab-plane in a direction perpendicular to dimers due to symmetry; there is a mirror plane including a dimer and a mirror plane perpendicular to a dimer (see inset to Fig. 1). A detailed analysis of the effect of intradimer DM interaction on the ESR line width [22]. Preliminary results suggest that this interaction is of about the same magnitude as the well-excepted interdimer interaction perpendicular to the plane. However, it has to be stressed that in addition to the calculation of the second moment, a detailed analysis of the exchange modulation frequency ω_{eff} is required since there is a high degree of frustration present in the system. Furthermore, the effect of additional DM interaction on the fine structure of single triplet excitations has to be considered carefully.

At the moment, the origin of the intradimer DM exchange interaction seems to some extent unclear. The buckling of the ab-planes is rather small as the bending angle of CuO_4 plaquettes amounts to 8° at room temperature [20]. This angle continuously drops towards 0° approaching the structural phase transition at 395 K so that in the high-temperature phase only the $D_\parallel$ interdimer component is again allowed in the static-lattice picture. However, as this interaction alone still does not allow an observation of singlet-triplet transitions in high-field ESR experiments, a DM interaction of a dynamical origin was proposed [23]. In this picture, lattice vibrations instantaneously break local symmetry allowing for the DM anisotropy. It seems that our ESR results would favor the dynamical mechanism, as there is only a small difference in the angular dependence of the line width at 295 and 525 K, i.e., at temperatures well below and well above the structural phase transition, respectively.

The effect of the buckling of the ab-planes on the anisotropy of the g-factor within the planes has also been considered. Since dimers are tilted by half the bending angle with respect to the c-axis (4° at room temperature), one can perform a rotation of the g-tensor of an individual dimer, whose principal axes are tilted due to buckling, into the crystal frame. This transformation yields two different components of the in-plane g-factor when the in-plane external magnetic field is applied, i.e., $g^a_\perp = (g^2_\perp \cos^2\theta + g^2_\parallel \sin^2\theta)^{1/2}$ for the case when the magnetic field is parallel to the dimer and $g^b_\perp = g_\perp$ for the magnetic field perpendicular to the dimer, where $g_\perp$ and $g_\parallel$ are the g-factor components in the eigenframe of the g-tensor. However, due to rather the small corrugation of the ab-planes, the effect is unobservably small as $g^a_\perp - g_\perp \approx 0.001$. This finding is consistent with almost no ϕ-dependence of the g-factor shown in Fig. 2.

3.4 Temperature Dependence of Line Widths

Finally, let us comment on the temperature dependence of the observed line width anisotropy (Fig. 3). The increase of the line width at 525 K with respect to room temperature is reverse to the behavior below room temperature, previously reported for a powdered sample [11]. However, a similar increase was also observed in a powdered sample when going beyond room temperature. The increase of the line width between 295 and 525 K in $\theta = 0°$ direction is virtually the same as in the case when the external field is applied in $\theta = 90°$ direction. Both directions yield 65 ± 5 G broader lines at 525 than at 295 K. Trying to give an explanation for such angular-independent behavior, or the observed line broadening in the first place, one can immediately exclude spin diffusion as the origin of the increase since the line shape remains “perfectly” Lorentzian even at 525 K. The next step would be the incorporation of static spin correlations, which

can play an important role in the temperature evolution of the line width in low-dimensional systems and can be sometimes seen in a rather broad temperature range between $T \geq J$ and $T \sim 10J$ [14]. Soos et al. [14] showed that including static spin correlations into an ordinary nn square lattice leads to the temperature-dependent second moment

$$M_2(J,T) = (M_2^{\mathrm{S}} F^{\mathrm{S}}(J,T) + M_2^{\mathrm{A}} F^{\mathrm{A}}(J,T)) \frac{\chi_{\mathrm{C}}}{\chi(T)}, \quad (9)$$

where indexes S and A stand for spin symmetric and spin antisymmetric contributions, respectively. The infinite-temperature second moments $M_2^{\mathrm{S,A}}$ are multiplied by functions describing temperature evolutions of static spin correlations $F^{\mathrm{S,A}}(J,T)$ and by the ratio between Curie-law susceptibility χ_{C} and the observed one $\chi(T)$. If the increase of the line width is due to static spin correlations, one will expect to observe an angular-dependent increase as the angular dependence is contained in the infinite-temperature second moments and is thus simply multiplied by corrections originating from static spin correlations. The calculation of $M_2(J,T)$ in the $SrCu_2(BO_3)_2$ system is more complicated due to the form of its Hamiltonian and a simple factorization into high-T second moment and a T-dependent function is not possible. However, one still expects to detect an angular-dependent increase, which is not experimentally observed [22]. Excluding also short-range order effects consequently indicates temperature-independent Line widths with the assumption of the pure spin Hamiltonian determining the spin dynamics.

Such temperature-independent behavior is often observed in magnetic crystals with significant exchange narrowing. It is then plausible that spin-phonon coupling has to be taken into consideration in the $SrCu_2(BO_3)_2$ system in order to account for the increase in the line width with the temperature. In fact, normal modes can modulate anisotropic spin interactions via spin-phonon interaction, which then induces transitions between energy levels of the system. The line width, regulated by the finite life-time of a spin in a particular energy level, is in this scenario expected to rise with temperature due to the increasing number of phonons. However, the A-term cannot entirely be of the dynamical origin as one might expect. Its increase between 295 and 525 K is too small with respect to the increase of the convex function describing the number of phonons that characterizes the direct phonon process [17, p. 112] of relaxation. Higher-order (Raman) phonon processes are expected to yield even faster temperature-dependent broadening of the line width with increasing temperature. Therefore we propose that the temperature-dependent part of the A-term is due to spin-phonon coupling, while its major (constant) part is due to magnetic anisotropy of DM origin. Spin-lattice coupling has indeed been reported to play a crucial role in a dramatic softening of the elastic constants in $SrCu_2(BO_3)_2$ [24]. It was suggested to be very strong and to be taken into consideration in any future model considering this particular system.

4 Conclusions

In summary, angular dependence of X-band ESR spectra of a $SrCu_2(BO_3)_2$ single crystal have been presented at two different temperatures. The magnetic anisotropy governing the spin dynamics has been shown to be quite substantial as the observed line widths are very broad in spite of the presence of strong isotropic exchange coupling. Among the possible anisotropy mechanisms the antisymmetric anisotropic DM interaction was determined as the only one capable of producing sufficiently large line widths. However, previously proposed interdimer DM exchange coupling, with DM vectors perpendicular to the crystal *ab*-plane, does not suffice for an adequate description of the experimentally observed angular dependence. In fact, sizable intradimer DM interaction has to be employed to provide a satisfactory explanation. Its origin, though, still remains unclear. It can be due to dynamical effects and/or is a fingerprint of buckling of the crystal *ab*-planes. In addition, the angular-independent increase of the line width with increasing temperature above room temperature suggests the presence of strong spin-phonon coupling in the system.

Acknowledgements

We thank the General Secretariat for Science & Technology (Greece) for the provision of financial support through a Greece-Slovenia Joint Research & Technology Program. A.L. and H.K. thank the Yamada Science Foundation (Japan) for supporting their work in low-dimensional materials.

References

1. Kageyama H., Yoshimura K., Stern R., Mushnikov N.V., Onizuka K., Kato M., Kosuge K., Slichter C.P., Goto T., Ueda Y.: Phys. Rev. Lett. **82**, 3168–3171 (1999)
2. Miyahara S., Ueda K.: Phys. Rev. Lett. **82**, 3701–3704 (1999)
3. Shastry B.S., Sutherland B.: Physica B **108**, 1069–1070 (1981)
4. Miyahara S., Ueda K.: J. Phys. Soc. Jpn. B **69**, 72 (2000)
5. Koga A.: J. Phys. Soc. Jpn. **69**, 3509–3512 (2000)
6. Kageyama H., Nishi M., Aso N., Onizuka K., Nukui K., Kodama K., Kakurai K., Ueda Y.: Phys. Rev. Lett. **84**, 5876–5879 (2000)
7. Nojiri H., Kageyama H., Onizuka K., Ueda Y., Motkawa M.: J. Phys. Soc. Jpn. **68**, 2906–2909 (1999)
8. Cépas O., Kakurai K., Regnault L.P., Ziman T., Boucher J.P., Aso N., Noshi M., Kageyama H., Ueda Y.: Phys. Rev. Lett. **87**, 167205 (2001)
9. Smith R.W., Keszler D.A.: J. Solid State Chem. **93**, 430–435 (1991)
10. Moriya T.: Phys. Rev. **120**, 91–98 (1960)
11. Zorko A., Arčon D., Lappas A., Giapintzakis J.: Phys. Rev. B **65**, 024417 (2001)
12. Kageyama H., Onizuka K., Yamauchi T., Ueda Y.: J. Cryst. Growth **206**, 65–67 (1999)
13. Kubo R., Tomita K.: J. Phys. Soc. Jpn. **9**, 888–919 (1954)
14. Soos Z.G., McGregor K.T., Cheung T.T.P., Silverstein A.J.: Phys. Rev. B **16**, 3036–3048 (1977)
15. Richards P.M.: Local Properties at Phase Transitions, p. 539. Amsterdam: North-Holland 1976.
16. Richards P.M., Salamon M.B.: Phys. Rev. B **9**, 32–45 (1974)

17. Pake G.E.: Paramagnetic Resonance. New York: W. A. Benjamin Inc. 1962.
18. Castner T.G., Seehra M.S.: Phys. Rev. B **4**, 38–45 (1974)
19. McGregor K.T., Soos Z.G.: J. Chem. Phys. **64**, 2506–2517 (1976)
20. Sparta K., Redhammer G.J., Roussel P., Heger G., Roth G., Lemmens P., Ionescu A., Grove M., Güntherodt G., Hüning F., Lueken H., Kageyama H., Onizuka K., Ueda Y.: Eur. Phys. J. B **19**, 507–516 (2001)
21. Kakurai K. in: Quantum Properties of Low-Dimensional Antiferromagnets (Ayiro A., Boucher J.P., eds.). Fukuoka: Kyushu University Press 2002.
22. Zorko A., Arčon D., van Tol H., Brunel L.C., Kageyama H.: Phys. Rev. B **69**, 174420 (2004)
23. Cépas O., Sakai T., Ziman T.: Prog. Theor. Phys. Suppl. **145**, 43–51 (2002)
24. Wolf B., Zherlitsyn S., Schmidt S., Lithi B., Kageyama H., Ueda Y.: Phys. Rev. Lett. **86**, 4847–4850 (2001)

Authors' address: Andrej Zorko, Jožef Stefan Institute, Jamova 39, 1000 Ljubljana, Slovenia
E-mail: andrej.zorko@ijs.si